

1 **Estimating biophysical and geometrical parameters of grapevine canopies (cv. Sangiovese) by**
2 **an unmanned aerial vehicle (UAV) and VIS-NIR cameras**

3

4 G. Caruso ¹⁾, L. Tozzini ¹⁾, G. Rallo ¹⁾, J. Primicerio ^{2,3)}, M. Moriondo ²⁾, G. Palai ¹⁾, R. Gucci ¹⁾

5

6 ¹⁾ Dipartimento di Scienze Agrarie, Alimentari e Agro-ambientali, Università di Pisa, Via del
7 Borghetto 80, 56124, Pisa, Italy

8 ²⁾ CNR-IBIMET– Consiglio Nazionale delle Ricerche, Istituto di Biometeorologia, via G. Caproni
9 8, 50145 Firenze, Italy

10 ³⁾ Dipartimento di Scienze Agrarie, Forestali e Agroalimentari, Università di Torino, Via Leonardo
11 Da Vinci 44, 10095 Grugliasco, Italy

12

13 **Summary**

14 Three zones of different vine vigour were identified in a mature vineyard (*Vitis vinifera* cv
15 Sangiovese) to test the potential of the Visible-Near Infrared (VIS-NIR) spectral information
16 acquired from an unmanned aerial vehicles (UAV) in estimating the leaf area index (LAI), leaf
17 chlorophyll, pruning weight, canopy height and canopy volume of grapevines. A significant linear
18 correlation between the normalized differential vegetation index (NDVI) and LAI or between NDVI
19 and leaf chlorophyll was found **at day of the year (DOY)** 162 and 190, whereas in August the
20 relationship between NDVI and leaf chlorophyll was less evident. The canopy volume of low-vigour
21 (LV) vines was 35 and 45% of the high-vigour (HV) and medium-vigour (MV) ones, respectively.
22 The pruning weight was linearly correlated with NDVI values of each vigour cohort. A good
23 correlation between the measured canopy volume and UAV-estimated one as well as between
24 measured and estimated canopy height was found. The combined use of VIS-NIR cameras and UAV
25 is a rapid and reliable technique to determine canopy structure and LAI of grapevine.

26

27 **Keywords:** canopy volume, greenness index, leaf area index, NDVI, remote sensing, structure from
28 motion, *Vitis vinifera* L.

29 **Introduction**

30 Precision viticulture (PV) relies on the understanding of inter and within-field variability to
31 define homogenous zones within the vineyard. This information is then used to optimize cultural
32 practices with the objective to achieve uniformity of growth and yield (Bramley et al., 2005; Arnò
33 et al., 2009). **Zoning in heterogeneous vineyards can be conducted** through the measurement and
34 geo-referencing of vine biophysical parameters, such as leaf area, vine vigour and leaf chlorophyll
35 content. These parameters are crucial for vineyard management as they are related to vegetative
36 growth, nutrient concentrations and water status of the vines. The Leaf Area Index (LAI) is related
37 to the surface responsible for solar radiation interception and gas exchange with the atmosphere
38 determining vine carbon assimilation, water consumption and potential productivity of vines. On a
39 practical level, LAI maps can be integrated and used in several agro-hydrological and crop models
40 developed to predict crop evapotranspiration, productivity and irrigation scheduling at field and
41 catchment scale (Minacapilli et al., 2009; Cammalleri et al., 2010). The LAI can be calculated by
42 either destructive sampling or indirect measurements, based on either hemispherical photography or
43 the transmittance of radiation through the vegetation (Lovell et al., 2003). Indirect methods are
44 currently preferred as they are less expensive and time consuming than destructive ones.

45 Measuring vine canopy volume and its variability within the vineyard is also important to
46 optimize canopy management (e.g. shoot positioning, shoot thinning, leaf removal, canopy hedging)
47 and pest control (spray application), especially when the variable rate techniques (VRT) are used
48 (Gil et al., 2007). Vine canopy volume can be calculated by manual measurements of height and
49 width, but this method is labour intensive and time consuming. Alternatively, by the use of mobile
50 terrestrial Light Detection and Ranging (Lidar) systems it is possible to create three-dimensional

51 models of the vineyard and estimate the grapevine canopy volume (Rossel et al., 2009). However,
52 these systems are still uncommon at the farm level due to their cost, especially when large areas are
53 to be scanned.

54 Vine vigour can be also inferred from measurements of pruning weight. The weight of the
55 pruned wood is related to the vegetative biomass produced during the growing season and, thus, to
56 the vine vigour (Dobrowski et al., 2003; Taylor and Bates, 2013). Pruning weight is also used to
57 express vine size in the parameterization of vine balance, as in the calculation of the Ravaz index,
58 commonly used by viticulturists to assess the relationship between vegetative and reproductive
59 activity. However, the Ravaz method is time consuming as it is necessary to measure many samples
60 and to interpolate data in order to draw a map of the vineyard vigour. The nitrogen (N) status is also
61 a valuable indicator of vigour and non destructive methods, based on either leaf reflectance or
62 transmittance responses, have been developed to estimate the leaf N concentration (Porro et al.,
63 2001; Brunetto et al., 2012). The greenness index calculated from SPAD readings using the Minolta
64 SPAD-502 (Minolta Corp., Ramsey, N.J.) has been often related to the leaf chlorophyll
65 concentration and to the total N content (Uddling et al., 2007). Because of the tight correlation
66 between chlorophyll and leaf nitrogen content, leaf chlorophyll can also be used as an indirect index
67 of the plant N status (Taskos et al., 2015). The ability to rapidly monitor the leaf chlorophyll content
68 during the entire growing season allows to promptly identify nitrogen deficiencies or excess in
69 vineyard. Since measurements are taken on single leaves, a drawback of this approach lies in the
70 large number of samples that are to be taken in space and time to fully cover a vineyard during the
71 growing season.

72 The Normalized Differential Vegetation Index (NDVI), one of the most commonly used
73 spectral indices in precision agriculture (Rouse et al., 1973), can also be used to estimate vigour. The
74 NDVI is widely used in proximal (both leaf and canopy scale) and remote (farm, district and regional
75 scale) sensing techniques (Matese et al., 2015). There are several reports that show that LAI and
76 vine size can be effectively estimated by using vegetative spectral indices derived from either

77 satellite or airborne multispectral images (Johnson et al., 2003; Hall et al., 2008; Dobrowsky et al.,
78 2003) although with less accuracy than when proximal sensing tools were used in the field or direct
79 measurements of pruning weight were taken (Stamatiadis et al., 2006; Taylor and Bates, 2012). It
80 has been recently shown that vegetative spectral indices acquired from unmanned aerial vehicles
81 (UAV) were very close to direct measurements of LAI and pruning weights in vineyards (Rey
82 Caramés et al., 2015). The UAV technique implies great flexibility in flight scheduling and low
83 operational costs (Primicerio et al., 2012; Matese et al., 2015), but there are few investigations so
84 far exploring the correlation between vine size and LAI using UAV. The increasing availability of
85 dedicated , low-cost, miniaturized sensors explain the interest in UAV for agricultural applications.
86 For instance, UAV equipped with multispectral cameras have been used to estimate vine
87 productivity and grape quality parameters (Fiorillo et al., 2012; Rey Caramés et al., 2015).

88 Recently, the acquisition of high resolution RGB images of the canopy from UAV joint to
89 Structure from Motion (SfM) technique has proved to be an effective tool for estimating plant
90 architecture through the computation of a Digital Surface Model (DSM) (Zarco-Tejada et al., 2014;
91 Torres-Sánchez et al., 2015; Ballesteros et al., 2015; Moriondo et al., 2016). However, to the best of
92 our knowledge no direct comparison between measured and estimated vine canopy volume has been
93 reported so far. Previous studies have used the SfM technique to create a 3-D vineyard point cloud
94 and to estimate vine canopy volume in order to predict vine LAI (Mathews et al., 2013; Ballesteros
95 et al., 2015), but the cross-validation of the canopy volume estimates through actual field
96 measurements was not conducted.

97 The general objective of this study was to test the ability of the VIS-NIR spectral information
98 acquired from an UAV to identify vines with different vigour in a Guyot-trained, mature vineyard
99 of cv. Sangiovese in Tuscany. Specific objectives were: a) to evaluate the capability of spectral
100 indices derived from an NIR-RG camera to estimate the LAI, the leaf chlorophyll concentration and
101 the vine pruning weight; b) to compare the values of canopy height and canopy volume estimated

102 from RGB images joint to the Structure from Motion technique with actual values measured in the
103 vineyard.

104

105 **Materials and methods**

106 *Plant material*

107 The experiments were carried out in a commercial vineyard (cv. Sangiovese, the most widely grown
108 cultivar in Italy) located at Suvereto in Tuscany (Italy, 43°04 N, 10° 41' E) in 2015-16. Vines were
109 planted in 1999 in a clay-loam soil at a 0.8 x 2.4 m spacing (North-South row orientation) and trained
110 according to the Guyot system. The vineyard was managed according to standard protocols for
111 organic viticulture, whereby the soil was tilled six times at a depth of 0.15 m from budburst through
112 harvest to control weeds. Composted sheep manure followed by the sowing of a cover crop (*Vicia*
113 *faba* L.) was applied after grape harvest. The technique of sexual confusion was used to control the
114 grapevine moth (*Lobesia botrana* Schiff.), whereas copper and sulphur compounds were sprayed
115 eight times during the growing season to control downy mildew (*Plasmopara viticola* Berk. & G.
116 Winter) and powdery mildew (*Uncinula necator* Schwein.), respectively. Shoot positioning and
117 lateral shoot removal were done at the beginning of July and repeated at the beginning of August,
118 when the crop was also manually adjusted to meet the standards for the local DOCG protocol for
119 high quality wines. At harvest (18 September) the average grape yield per vine was 1.2 kg. Annual
120 and summer (21 June – 21 September) precipitations were 809 and 39 mm, respectively. Summer
121 mean temperature was 24.0 °C, and the highest daily mean temperature (29.1 °C) was recorded on
122 8 August.

123 Three homogeneous zones of high (HV), medium (MV) and low (LV) vigour were identified
124 on the basis of the Normalized Different Vegetation Index (NDVI) calculated from multispectral
125 images acquired during a preliminary UAV survey in May (DOY 149) (Fig. 1A). The Iterative Self-
126 Organizing Data Analysis Technique (ISODATA), implemented in ArcGIS software (ESRI,
127 Redlands, Ca, USA), was used to set the boundaries of the three zones within the vineyard.

128 Within each homogeneous zone a group of 75 vines, consisting in three adjacent portions of
129 row (20 m each), was used for field measurements of the Leaf Area Index, leaf chlorophyll and
130 canopy volume. All three rows were included in LAI measurements, as reported in the following
131 section, while only the central row, consisting in four adjacent replicates of 4 m each (the first and
132 the last 0.5 m of each replicate were excluded), was used for the determinations of canopy height,
133 canopy width, canopy volume, leaf chlorophyll, and pruning weight.

134

135 *LAI, leaf chlorophyll, canopy volume, pruning weight*

136 The LAI was measured not destructively at DOY 162 and 190 by a LAI-2000 optoelectronic
137 sensor (LI-COR, Lincoln, Nebraska, USA). Due to the heterogeneous structure of the canopies
138 arranged in rows, a tow-azimuth protocol was followed (Welles and Norman, 1991; LI-COR 1992).
139 Initially, an ambient light standardization was carried out with the sensor extended upward and over
140 the top of the canopy. Four below-canopy measurement were then recorded along a diagonal transect
141 pointed toward the middle of the central row of each plot, with the instrument held a few centimeters
142 above the soil. The first reading was taken directly beneath the mid-point of the central row, whereas
143 the next three measurements were taken one-quarter, one-half and three-quarters of the distance from
144 the adjoining row. This procedure was repeated for a total of four transects per plot in order to record
145 both sides of the central row of the investigated plot. A physical cap was used to limit the azimuthal
146 field-of-view to 180°, facing away from the operator and the adjoining row of vines.

147 A sample of 30 leaves with variable greenness index was selected at veraison (DOY 220) to
148 determine the correlation between SPAD readings (greenness index) and the actual chlorophyll
149 concentration. Chlorophyll was extracted using N,N-dimethylformamide according to the method
150 described by Moran and Porath (1980), and total chlorophyll (a+b) concentration (mg/dm² of leaf
151 area) calculated based on the equations provided by Lichtenthaler and Wellburn, (1983). The
152 greenness index was measured on 11 June (DOY 162), 9 July (DOY 190) and 12 August (DOY 224)
153 on 15 fully-expanded leaves for each replicate using a Minolta SPAD 502 portable greenness meter

154 (Konica Minolta, Inc., Osaka, Japan). In particular, measurements were taken on leaves (three
155 measurements per leaf) inserted on the basal, median and apical shoot zone (located at a height from
156 the ground of 0.90, 1.25 and 1.60 m, respectively) and repeated at regular intervals (1 m) along the
157 block central row, excluding the first and the last 0.5 m of each of the four replicates (Fig. 1B). The
158 greenness index confirmed to be a reliable proxy of chlorophyll concentration per unit of leaf area
159 ($y = 0.002 x^2 + 0.051 x$; $R^2 = 0.90$) (Supplemental Fig. 1). This equation was then used to convert
160 the greenness index values into leaf chlorophyll concentrations.

161 Following the same sampling protocol used for the greenness index determinations, the
162 maximum canopy height, canopy height from the ground and canopy width were measured on 16
163 July (DOY 197). These data were used to create a 2-D canopy silhouette at 1 m intervals and then,
164 the LOFT command implemented in AutoCAD (Autodesk Inc., McInnis Parkway, San Rafael, CA,
165 USA) was used to obtain a 3-D canopy model of each replicate (Fig. 1B).

166 In February 2016 the pruning wood removed from each of the four replicates per vigour
167 group was weighed and expressed as kilograms per linear meter of vine-row.

168

169 *UAV setting and multispectral images collection*

170 The acquisition campaign was performed using a S1000 UAV octocopter (DJI, Shenzhen,
171 China) able to fly autonomously over a predetermined waypoint course. The S1000 was equipped
172 with a 2-axis stabilized gimbal equipped with a consumer photo-camera (RGB) and a multispectral
173 camera (NIR-RG). The RGB camera was a Coolpix P7700 (Nikon, Shinjuku, Japan) embodying a
174 12.2-megapixel CMOS sensor, whereas the NIR-RG multispectral camera was the Tetracam ADC-
175 lite (Tetracam, Inc., Gainesville, FL, USA) equipped with a 3.2-megapixel CMOS sensor. Images
176 were acquired at noon under clear sky conditions, the flight altitude was 100 m above ground level
177 (AGL) at a UAV flight speed of 4 m s^{-1} , and the ground sample distance (GSD) was 4.02 cm. The
178 image forward and side overlap (80% and 70%, respectively), guaranteed an optimal
179 photogrammetric processing. Images were recorded in the visible green (G) and red (R) and near

180 infrared (NIR) domain with nominal **bandwidth** of 520–600, 630–690, and 760–900 nm,
181 respectively. Four flights were made at DOY 149 (29 May), DOY 162, DOY 190 and DOY 224,
182 corresponding to the BBCH-scale stages 61 (beginning of flowering), 71 (fruit set completed), 77
183 (beginning of bunch closure) and 83 (veraison, berries developing color) (Lorenz et al, 1995). In
184 order to standardize the radiation conditions, a white reference panel was acquired inside the target
185 of the multispectral images just before each flight. An additional flight was made on 16 July (DOY
186 197) at an altitude of 50 m AGL and RGB images were acquired and processed for the 3D canopy
187 reconstruction (**GSD of 1.54 cm**). At the same date, before the UAV flight, a set of sixty ground
188 control points were placed in the vineyard and georeferenced using a Leica GS09 real time kinematic
189 GPS (Leica Geosystems A.G., Heerbrugg, Switzerland) able to achieve a 3D resolution of 0.02 m.

190

191 *Images processing*

192 The multispectral images were first mosaicked using Autopano Giga 3.5 Software (Kolor
193 SARL, Challes-les-Eaux, France), then georeferenced and orthorectified by using the known **ground**
194 **control points** (ArcGIS software®, ESRI, Redlands, CA, USA). The absence of vegetation cover in
195 the inter-row space, due to the periodic soil disking, allowed to obtain a clear separation of soil and
196 canopy pixels in the orthomosaic and, thus, a precise extraction of the vegetation spectral
197 information was possible. The Normalized Difference Vegetation Index (NDVI; Rouse et al., 1974),
198 was calculated by means of the map algebra technique implemented in ArcGIS software (ESRI,
199 Redlands, Ca, USA).

200 The three-dimensional canopy volume of grapevines was reconstructed starting from the
201 digital surface model (DSM) obtained using a structure from motion approach (SfM). According to
202 the SfM pipeline, in the first step an algorithm tracks a set of points common to several overlapping
203 images. The 3D positions of every identified key points was then estimated along with camera
204 position and its orientation for every picture. The estimated camera positions and digital images were
205 further processed to retrieve the positions of non-feature point pixels that were finally combined into

206 a single dense point cloud. In our specific case, RGB images acquired by UAV on DOY 197 were
207 used as input Agisoft Photo-Scan® (Agisoft LLC). Three-dimensional structures were obtained as
208 a point cloud and were further processed and rasterized to retrieve canopy height above the ground.
209 The point clouds obtained were firstly rescaled and georeferenced using the spatial coordinates
210 (UTM 32N) of the sixty ground control points previously placed on the study area and the relevant
211 point clouds were then clipped strictly around the vineyard under study. The density of these point
212 clouds was 8.500.000 points over a surface of 0.5 ha. The DSM generated from the point cloud was
213 then processed in ArcGIS to obtain a digital terrain model (DTM) of the vineyard to retrieve the
214 height of each three-dimensional axes of the canopy point above the ground.

215 The DSM generated from the point cloud was then processed in ArcGIS to obtain a digital
216 terrain model (DTM) of the vineyard. A raster consisting only in the pixels of the canopy vines was
217 obtained by subtracting the DTM to DSM using the map algebra technique. The maximum canopy
218 height was obtained from the corresponding pixel of each replicate. The vine canopy volume was
219 obtained by integrating the volume of all the pixel located below the canopy: the height and the area
220 of each pixel was multiplied to obtain the pixel volume; the volume occupied by the vine was
221 calculated by adding the volume of each pixel below the canopy. Canopy volume was calculated as
222 the difference between total volume of each replicate and: a) the volume comprised between the
223 ground and the first wire (0.9 m from the ground); b) the volume comprised between the ground and
224 the measured distance from the ground of the canopy of each replicate.

225

226 *Statistical analysis*

227 Means of the various measured parameters of the three vines groups (HV, MV and LV) were
228 separated by least significant differences (LSD) at $p \leq 0.05$ after analysis of variance (ANOVA).
229 Where applicable, linear regression analysis was conducted using Costat (CoHort Software,
230 Monterey, USA).

231

232 **Results and discussion**

233 The leaf chlorophyll tended to increase between June (DOY 162) and July (DOY 190) in all
234 the three groups of vine vigour. While this trend continued for LV vines in August (DOY 224), the
235 leaf chlorophyll decreased (MV vines) or remained stable for HV ones (Fig. 2A). Leaf chlorophyll
236 was significantly lower in LV vines than the other two vigour cohorts in June and July, whereas the
237 MV vines showed the lowest values in August.

238 The NDVI of the three vigour cohorts were significantly different for NDVI at DOY 149,
239 with the higher and lowest values measured in HV and LV vines, respectively. Starting from DOY
240 162 the NDVI of MV vines became similar to that of HV ones, and at DOY 224 differences between
241 the three groups had disappeared (Fig. 2B). The lack of differences in NDVI values between groups
242 in August was probably due to the canopy manipulations (shoot thinning and shoot positioning)
243 performed in July. A similar pattern was observed for NDVI of the HV and MV vines, with values
244 that increased between May (DOY 149) and June (DOY 162) and then remained approximately
245 constant until August (DOY 224). The seasonal course of NDVI for HV and MV vines was similar
246 to that reported by other authors (Johnson et al., 2003), with NDVI that progressively increased up
247 to mid-June to remain stable, or slightly decreasing, in the summer. In contrast, an almost linear
248 increase in NDVI values between May and August was observed in the LV vines (Fig. 2B),
249 paralleling the course of SPAD readings. The pattern of NDVI for LV vines can be probably
250 explained by the location was different because they were located in an area subjected to
251 waterlogging during the winter, which depressed vegetative growth in spring and resulted in more
252 prolonged vegetative activity in the summer than the other groups. The steady increase of leaf
253 chlorophyll in LV vines between June and August seems to confirm this hypothesis. Differences in
254 leaf chlorophyll content reflecting differences in soil water availability conditions has been
255 previously reported in grapevines (Bertamini et al., 2006).

256 A linear correlation between leaf chlorophyll and NDVI was found at DOY 162 and 190,
257 whereas at DOY 224 there was no significant correlation (Fig. 3). Similarly, a wider range of leaf

258 chlorophyll values was observed in June (from 3.0 to 4.7 mg dm⁻²) and July (from 3.4 to 5.3) when
259 the canopy was still actively growing, than in August (from 4.2 to 5.0), after the canopy had been
260 hedged and grapes were beginning to ripe. The basal, median and apical leaves differently
261 contributed to the general NDVI-leaf chlorophyll relationship at the canopy level. The chlorophyll-
262 NDVI (whole-canopy) relationship was always tighter for basal leaves ($R^2 = 0.66^{**}$, 0.66^{**} and
263 0.37^* at DOY 162, 190 and 224, respectively) than that for median or apical ones (Supplemental
264 Fig. 3). Since basal leaves are commonly sampled to determine whole vine nutrient status (Romero
265 et al. 2010), the above relationships can be used to rapidly estimate the chlorophyll or the nitrogen
266 status of vines at the field level (Steele et al., 2008; Taskos et al., 2015). The seasonal course of leaf
267 chlorophyll in leaves located in the basal, median and apical part of the shoot were different.
268 Regardless of the vigour cohorts, leaf chlorophyll tended to increase in apical leaves from June
269 (DOY 162) through August (DOY 224), whereas an opposite trend was observed in basal leaves.
270 Similar results were observed in previous studies conducted on the same cultivar as a result of leaf
271 aging (Poni et al., 1994). At the last date of measurement (DOY 224) significant differences between
272 basal, median and apical leaves were measured in LV vines, but in MV and HV ones (Supplemental
273 Fig. 2).

274 A significantly linear NDVI-LAI relationship ($R^2=0.88$) was found (Fig. 4), similarly to
275 results reported in another study where NDVI values were calculated from multispectral satellite
276 images (Johnson et al., 2003). Hall et al. (2008) reported a closer relationship between vine canopy
277 area and LAI ($R^2=0.83$) than that between NDVI and LAI ($R^2=0.74$), when data of three
278 phenological stages (post-budburst, post-flowering and veraison) were considered. Moreover, when
279 the data were separated according to phenological stages the NDVI-LAI relationship was significant
280 only at veraison.

281 The weight of pruning wood, commonly used as an estimate of vine vigour, matched the
282 vegetative vigour initially identified on the basis of the NDVI determinations (0.54, 0.41 and 0.28
283 kg m⁻¹ for HV, MV and LV cohorts, respectively) and was indeed linearly correlated with NDVI

284 values of each group (Fig. 5). The pruning weights in our study were consistent with those reported
285 by Taylor and Bates (2013) (0.54, 0.46 and 0.39 kg m⁻¹ for HV, MV and LV, respectively) and
286 slightly higher than those reported by Fiorillo et al. (2012) (0.39, 0.22 and 0.20 kg m⁻¹). The
287 correlation between the pruning wood and NDVI values measured at DOY 149, 162, 190 and 224
288 was always significant and the coefficient of determination increased from May to August ($R^2 =$
289 0.47, 0.56, 0.73 and 0.83 for DOY 149, 162, 190 and 224, respectively) (Fig. 5). Bonilla et al. (2015)
290 also found a significant relationship between NDVI measured in August and pruning weight.
291 Dobrowski et al. (2003) reported a positive and linear correlation between the ratio vegetation index
292 ($RVI = NIR/Red$), calculated from multispectral airborne images acquired in August (post-veraison),
293 and the pruning weight (values between 0.2 to 1.2 kg m⁻¹).

294 The vine canopy volume reflected the vigour of each group. In particular, the canopy volume
295 of LV vines was 35 and 45% that of HV and MV ones, respectively. A good correlation between the
296 measured canopy volume and the UAV estimated one was found. When a constant height of 0.9 m
297 (the height of the first wire above ground) was used for the canopy volume estimation the data points
298 were distributed along a 1:1 line ($R^2 = 0.62$ and $RMSE = 0.08$) and there was a linear relationship
299 between estimated and measured canopy volume (Fig. 6A). The coefficient of determination
300 increased ($R^2 = 0.75$) when the actual distance of the canopy from the ground was used in the
301 calculations, but in this case the estimated canopy volume diverged from the 1:1 line (Fig. 6B). The
302 variability of those relationships depends on the width and geometry of the canopy since the point
303 cloud method includes an additional volume below the maximum width of the canopy: the higher
304 the maximum width of the canopy, the larger the overestimation of canopy volume below that width.
305 When the actual distance from the ground is used (Fig. 6C), the lowest portion of the canopy volume
306 (grey area) is included in the canopy volume calculation, resulting in a higher value of R^2 .
307 Concomitantly, the approximation to a rectangular shape of the section comprised between the 0.9
308 m and the measured height from the ground leads to the inclusion of an additional volume (dotted
309 area) which in turn, leads to an overestimation of canopy volume (Fig. 6C). Therefore, using a fixed

310 height of the canopy from the ground (first wire) for canopy volume determination is a better option
311 for applications at vineyard scale. The estimated values of the maximum canopy height were close
312 to the ones measured manually in the field (RMSE=0.15) and the relationship between measured
313 and UAV-estimated values was linear ($R^2=0.75$) (Fig. 7). Zarco-Tejada et al. (2014) quantified the
314 height of olive trees using high resolution images acquired from UAV and evaluated the effect of
315 the spatial resolution of the input images on the RMSE of the measured/estimated tree height
316 relationship. In particular, they reported RMSE values of 0.33 and 0.60 m when the images used for
317 to generate the DSM had spatial resolution of 0.05 and 0.50 m pixel⁻¹, respectively. Torres-Sánchez
318 et al. (2015) reported a coefficient of determination of 0.65 (UAV flight altitude of 50 m) and 0.63
319 (UAV flight altitude of 100 m) for the relationship between measured and estimated canopy volume
320 of olive trees.

321 The maps of pruning weight, LAI and canopy volume, derived from the specific relationships
322 between NDVI and each of these variables, are important inputs for different variable rate
323 applications concerning canopy, irrigation and pest management. The estimation of the pruning
324 weight at field scale may facilitate pruning and thinning strategies and, thus, optimize the vine
325 vegetative and reproductive balance. At the same time, LAI maps allow to better estimate vine water
326 requirements and to increase water use efficiency. In fact, vine water use and crop coefficient, the
327 latter used to calculate the crop evapotranspiration (ET_c), have been shown to be closely related to
328 leaf area per vine and LAI (Williams and Ayars, 2005; Netzer et al., 2008). The maps of canopy
329 volume, as well as LAI maps, can be used in the variable rate spraying applications allowing to
330 optimize the applied doses of pesticides or fertilizer according to the vine canopy volume in each
331 area, with relevant benefits in terms of environmental sustainability, food security and cost reduction
332 (Zaman et al., 2005; Gil et al., 2007).

333 In conclusion, the results presented in this work show the potential of the multispectral and
334 RGB imagery from UAV to determine some biophysical and geometrical characteristics of
335 grapevines. The NDVI derived from multispectral camera allowed to identify zones of different vine

336 vigour within the vineyard and to estimate accurately leaf chlorophyll, LAI and pruning weight, with
337 potential positive effects on grapevine nutrition, irrigation and canopy management. The major
338 contribution of the basal leaves to the general NDVI (whole canopy)-leaf chlorophyll relationship
339 confirms the potential in the use of the multispectral imagery from UAV for the determination of
340 vine nitrogen status. We also showed that UAV-derived techniques can be used for low-cost, reliable
341 determinations of canopy structure. The lack of information on canopy geometry and LAI is still the
342 limiting factor to understand whole-vine physiological processes like photosynthesis and
343 evapotranspiration in the field. In addition, optimizing cultural practices requires quick methods to
344 determine spatial variability within the vineyard. Current management to modern vineyards is highly
345 intense and, therefore, we need tools and techniques that allow to estimate and model functional
346 activities at the whole vine and vineyard level rather than analysing processes in single leaves or
347 canopy parts only. In this respect, we report that the RGB consumer camera mounted on UAV can
348 be used to reconstruct a realistic 3-D model of the canopy in vertical training systems and estimate
349 canopy volumes of vertically trained (Guyot) vines. However, further investigations are need to
350 verify the reliability of this technique for other training systems like GDC, Lyre or tendons where
351 the canopy has a more horizontal display.

352

353 **Acknowledgemnts**

354 We are grateful to the Bulichella farm for hosting the trials. Research supported by the FARFALLA
355 project, PRAF 2012-2015 (Identification, valorization and conservation of plants and crops in
356 Southern-Central Tuscany).

357

358 **References**

359 Arnó, J.; Martínez Casasnovas, J. A.; Ribes Dasi, M.; Rosell, J. R.; 2009: Review. Precision
360 viticulture. Research topics, challenges and opportunities in site-specific vineyard
361 management. Span. J. Agric. Res., 7(4), 779-790.

362 Ballesteros, R.; Ortega J. F.; Hernández D.; Moreno M. A.; 2015: Characterization of *Vitis vinifera*
363 L. Canopy Using Unmanned Aerial Vehicle-Based Remote Sensing and Photogrammetry
364 Techniques. *Am J Enol Vitic* **66**, 120-129.

365 Bertamini, M.; Zulini L.; Muthuchelian K.; Nedunchezian N.; 2006: Effect of water deficit on
366 photosynthetic and other physiological responses in grapevine (*Vitis vinifera* L. cv. Riesling)
367 plants. *Photosynthetica* **44**, 151-154.

368 Bonilla, I.; de Toda F. M.; Martínez-Casanovas, J. A.; 2015: Vine vigor, yield and grape quality
369 assessment by airborne remote sensing over three years: Analysis of unexpected
370 relationships in cv. Tempranillo. *Span. J. Agric. Res.* **13**, 1-8.

371 Bramley, R. G. V.; 2005: Understanding variability in winegrape production systems. 2. Within
372 vineyard variation in quality over several vintages. *Aust. J. Grape Wine Res.* **11**, 33-42.

373 Brunetto, G.; Trentin, G.; Ceretta, C. A.; Giroto, E.; Lorensini, F.; Miotto, A.; Moser, G. R. Z.; de
374 Melo, G. W.; 2012: Use of the SPAD-502 in estimating nitrogen content in leaves and
375 grape yield in grapevines in soils with different texture. *Am. J. Plant. Sci.* **3**, 1546-1561.

376 Cammalleri, C.; Agnese, C.; Ciraolo, G.; Minacapilli, M.; Provenzano, G.; Rallo, G.; 2010: Actual
377 evapotranspiration assessment by means of a coupled energy/hydrologic balance model:
378 Validation over an olive grove by means of scintillometry and measurements of soil water
379 contents. *J. Hydrol.* **392**, 70-82.

380 Dobrowski, S. Z.; Ustin, S. L.; Wolpert, J. A.; 2003: Grapevine dormant pruning weight prediction
381 using remotely sensed data. *Aust. J. Grape Wine Res.* **9**, 177-182.

382 Fiorillo, E.; Crisci, A.; De Filippis, T.; Di Gennaro, S. F.; Di Blasi, S.; Matese, A.; Primicerio, J.,
383 Vaccari, F. P.; Genesio, L.; 2012: Airborne high-resolution images for grape classification:
384 changes in correlation between technological and late maturity in a Sangiovese vineyard in
385 Central Italy. *Aust. J. Grape Wine Res.*, **18**, 80-90.

- 386 Gil, E.; Escolà, A.; Rosell, J. R.; Planas, S.; Val, L.; 2007: Variable rate application of plant protection
387 products in vineyard using ultrasonic sensors. *Crop Prot.* **26**(8), 1287–1297.
- 388 Hall, A.; Louis, J.P.; Lamb, D.W.; 2008: Low-resolution remotely sensed images of winegrape
389 vineyards map spatial variability in planimetric canopy area instead of leaf area index. *Aust.*
390 *J. Grape Wine Res.* **14**, 9–17.
- 391 Johnson, L.F.; 2003: Temporal stability of an NDVI-LAI relationship in a Napa Valley vineyard.
392 *Aust. J. Grape Wine Res.* **9**, 96-101.
- 393 Lichtenthaler, H. K.; Wellburn, A. R.; 1983: Determinations of total carotenoids and chlorophylls a
394 and b of leaf extracts in different solvents. *Biochem. Soc. Trans.* **11**, 591–592.
- 395 Lorenz, D. H.; Eichorn, K. W.; Bleiholder, H.; Klose, R.; Meier, U.; Weber, E.; 1995: Phenological
396 growth stages of the grapevine (*Vitis vinifera* L. ssp. *vinifera*)—Codes and descriptions
397 according to the extended BBCH scale. *Aust. J. Grape Wine Res.* **1**, 100–103.
- 398 Lowell, J.; Jupp, D.; Culvenor, D.; Coops, N.; 2003: Using airborne and ground-based ranging
399 LIDAR to measure canopy structure in Australian forests. *Can. J. Rem. Sens.* **29**(5): 607-
400 622.
- 401 Matese, A.; Toscano, P.; Di Gennaro, S. F.; Genesio, L.; Vaccari, P.; Primicerio, J.; Belli, C.; Zaldei,
402 A.; Bianconi, R.; Gioli, B.; 2015: Intercomparison of UAV, aircraft and satellite remote
403 sensing platforms for precision viticulture. *Remote Sens.* **7**, 2971-2990.
- 404 Mathews, A. J.; Jensen, J. L. R.; 2013: Visualizing and quantifying vineyard canopy LAI using an
405 unmanned aerial vehicle (UAV) collected high density structure from motion point cloud.
406 *Remote Sens.* **5**(5), 2164-2183.

407 Moriondo, M.; Leolini, L.; Staglianò, N.; Argenti, G.; Trombi, G.; Brilli, L.; Dibari, C.; Leolini, C.;
408 Bindi, M.; 2016: Use of digital images to disclose canopy architecture in olive tree, *Scientia*
409 *Horticulturae* **209**, 1-13, doi <http://dx.doi.org/10.1016/j.scienta.2016.05.021>.

410 Moran, R.; Porath, D.; 1980: Chlorophyll determinations in intact tissue using N,N-
411 dimethylformamide. *Plant Physiol.* **65**, 478–479.

412 Netzer, Y.; Yao, C.; Shenker, M.; Bravdo, B. A.; Schwartz, A.; 2009: Water use and the development
413 of seasonal crop coefficients for Superior Seedless grapevines trained to an open-gable trellis
414 system. *Irrig. Sci.* **27**, 109–120.

415 Poni, S.; Intrieri, C.; Silvestroni, O.; 1994: Interactions of leaf age, fruiting, and exogenous
416 cytokinins in Sangiovese grapevine under non-irrigated conditions. II. Chlorophyll and
417 nitrogen content. *Am. J. Enol. Vitic.* **45**, 278-284.

418 Porro, D.; Dorigatti, C.; Stefanini, M.; Ceschini, A.; 2001: Use of SPAD Meter in Diagnosis of
419 Nutritional Status in Apple and Grapevine. *Acta Hort.* **564**, 243-252.

420 Primicerio, J.; Di Gennaro, S.F.; Fiorillo, E.; Genesio, L.; Lugato, E.; Matese, A.; Vaccari, F. P.;
421 2012: A flexible unmanned aerial vehicle for precision agriculture. *Precis. Agric.* **13**, 517–
422 523.

423 Rey-Caramés, C., Diago, M. P.; Martín, M. P.; Lobo, A., Tardaguila, J.; 2015: Using RPAS multi-
424 spectral imagery to characterise vigour, leaf development, yield components and berry
425 composition variability within a vineyard. *Remote Sens.* **7**(11), 14458-14481.

426 Romero, I.; García-Escudero, E.; Martín, I.; 2010: Effects of leaf position on blade and petiole
427 mineral nutrient concentration of Tempranillo grapevine (*Vitis vinifera* L.). *Am. J. Enol.*
428 *Vitic.* **61**, 544-550.

429 Rosell, J.R.; Llorens, J.; Sanz, R.; Arno, J.; Ribes-Dasi, M.; Masip, J.; Escola, A.; Camp, F.;
430 Solanelles, F.; Gracia, F.; 2009: Obtaining the three-dimensional structure of tree orchards
431 from remote 2D terrestrial LIDAR scanning. *Agr. For. Meteorol.* **149**, 1505–1515.

432 Rouse Jr., J.W.; Haas, R. H.; Schell, J. A.; Deering, D. W.; 1973: Monitoring vegetation systems in
433 the great plains with ERTS. In: *Proceedings of the Third ERTS Symposium*, NASA SP-351
434 1. US Government Printing Office, Washington, DC, pp. 309–317.

435 Stamatiadis, S; Taskos, D.; Tsadilas, C.; Christofides, C.; Tsadila, E.; Schepers, J.S.; 2006: Relation
436 of ground-sensor canopy reflectance to biomass production and grape color in two merlot
437 vineyards. *Am. J. Enol. Vitic.* **57**(4), 415-422.

438 Steele, M. R.; Gitelson, A.; Rundquist, D. C.; 2008: A comparison of two techniques for
439 nondestructive measurement of chlorophyll content in grapevine leaves. *Agron. J.* **3**, 779-
440 782.

441 Taylor, J. A.; Bates, T. R.; 2012: Sampling and estimating average pruning weights in concord
442 grapes. *Am. J. of Enol. Vitic.* **63**, 559-563.

443 Taylor, J. A.; Bates T. R.; 2013: Temporal and spatial relationships of vine pruning mass in Concord
444 grapes. *Aust. J. Grape Wine Res.* **19**, 401–408.

445 Taskos; D. G.; Koundouras, S.; Stamatiadis, S.; Zioziou, E.; Nikolau, N.; Karakioulakis, K.,
446 Theodorou, N.; 2015: Using active canopy sensors and chlorophyll meters to estimate
447 grapevine nitrogen status and productivity. *Precision Agric.* **16**, 77-98.

448 Torres-Sánchez, J.; López-Granados, F.; Serrano, N.; Arquero, O.; Peeña, J.; 2015: High-throughput
449 3-D monitoring of agricultural-tree plantations with unmanned aerial vehicle (UAV)
450 technology. *PLoS ONE* **10**(6): e0130479. doi:10.1371/journal.pone.0130479.

451 Uddling, J.; Gelang-Alfredsonn, J.; Piikki, K.; Pleijel, H.; 2007: Evaluating the relationship between
452 leaf chlorophyll concentration and SPAD-502 chlorophyll meter readings. *Photosynth. Res.*,
453 **91**, 37-46.

454 Vitale, L.; Di Tommasi, P.; D'Urso, G.; Magliulo, V.; 2016: The response of ecosystem carbon
455 fluxes to LAI and environmental drivers in a maize crop grown in two contrasting seasons.
456 *Int. J. Biometeorol.* **60**, 411- 420.

457 Wells, J. M.; J. M. Norman; 1991: Instrument for indirect measurement of canopy architecture.
458 *Agron. J.* **83**, 818 - 825.

459 Williams, L. S.; Ayars, J. E., 2005: Grapevine water use and crop coefficient are linear functions of
460 the shaded area measured beneath the canopy. *Agric. For Meteorol.* **132**, 201–211.

461 Zaman, Q.; Schumann, A.W.; Miller, W. M., 2005: Variable rate nitrogen application in Florida
462 citrus based on ultrasonically sensed tree size. *Appl. Eng. Agric.* **21**, 331–335.

463 Zarco-Tejada, P. J.; Diaz-Varela, R.; Angileri, V.; Loudjani, P.; 2014: Tree height quantification
464 using very high resolution imagery acquired from an unmanned aerial vehicle (UAV) and
465 automatic 3D photo-reconstruction methods. *Eur. J. Agron.* **55**, 89-99.

466

467

468

469

470

471

472

473 **Captions for figures**

474 Fig. 1. Normalized difference vegetation index (NDVI) map (DOY 149) including the three groups
475 of vines (cv. Sangiovese) used for field measurements (A) and three-dimensional canopy
476 models of High (HV), Medium (MV) and Low Vigor (LV) vines produced from measurement
477 taken in the field at DOY 197 (B). Dots indicate the positions at which canopy width and leaf
478 chlorophyll were measured.

479 Fig. 2. Seasonal courses of leaf chlorophyll content (A) and NDVI (B) in high (HV), medium (MV)
480 and low (LV) vigour grapevines (cv. Sangiovese). Values are means – SD of four replicates
481 for each group.

482 Fig. 3. The relationship between NDVI and leaf chlorophyll in high (HV), medium (MV) and low
483 (LV) vigour grapevines (cv. Sangiovese) at DOY 162 (A), 190 (B) and 224 (C). In D data
484 from all dates of measurement were pooled together. Each symbol represents one replicate.
485 Linear regression equations: (A) $y = 7.74 x + 0.88$; $R^2 = 0.73$; (B) $y = 11.1 x - 0.17$; $R^2 =$
486 0.74 ; (D) $y = 9.2 x + 0.55$; $R^2 = 0.61$;

487 Fig. 4. The relationship between NDVI and LAI values in high (HV), medium (MV) and low (LV)
488 vigour grapevines (cv. Sangiovese) at DOY 162 and 190. Each symbol represents one
489 replicate. Linear regression equation: $y = 4.62 x - 1.22$; $R^2 = 0.88$.

490 Fig. 5. The relationship between NDVI measured at DOY 149 (A), 162 (B), 190 (C) and 224 (D) in
491 2015 in high (HV), medium (MV) and low (LV) vigour grapevines and pruning wood
492 weighted on 19 February 2016. Each symbol represents one replicate. Linear regression
493 equations: $y = 2.34x - 0.46$, $R^2 = 0.47$, 0.015* (A); $y = 2.04x - 0.41$, $R^2 = 0.62$, 0.003** (B);
494 $y = 2.65x - 0.69$, $R^2 = 0.82$, 0.000*** (D); $y = 4.00x - 1.30$, $R^2 = 0.83$, 0.000*** (D).

495 Fig. 6. Comparison between ground measured and UAV-estimated canopy volume (of a 1-m
496 vineyard row) in high (HV), medium (MV) and low (LV) vigour grapevines at DOY 197.

497 The UAV-estimated canopy volumes were obtained by considering a distance of the canopy
498 from the ground of 0.9 m (height of the first wire) (A) or by using the distance measured for
499 each replicate (B). Each symbol represents one replicate. The solid line is the fitted linear
500 function and the dotted one is the 1:1 line. A simplified canopy longitudinal section is also
501 reported (C). Horizontal lines (0.9, 1.25, 1.60 m) indicate the height of the three wires at
502 which the canopy width was measured.

503 Fig. 7. Comparison between ground measured and UAV-estimated canopy height values in high
504 (HV), medium (MV) and low (LV) vigour grapevines at DOY 197. Each symbol represents
505 one replicate. The solid line is the fitted linear function and the dotted line is the 1:1 line.

506

507

508

509

510

511

512

513

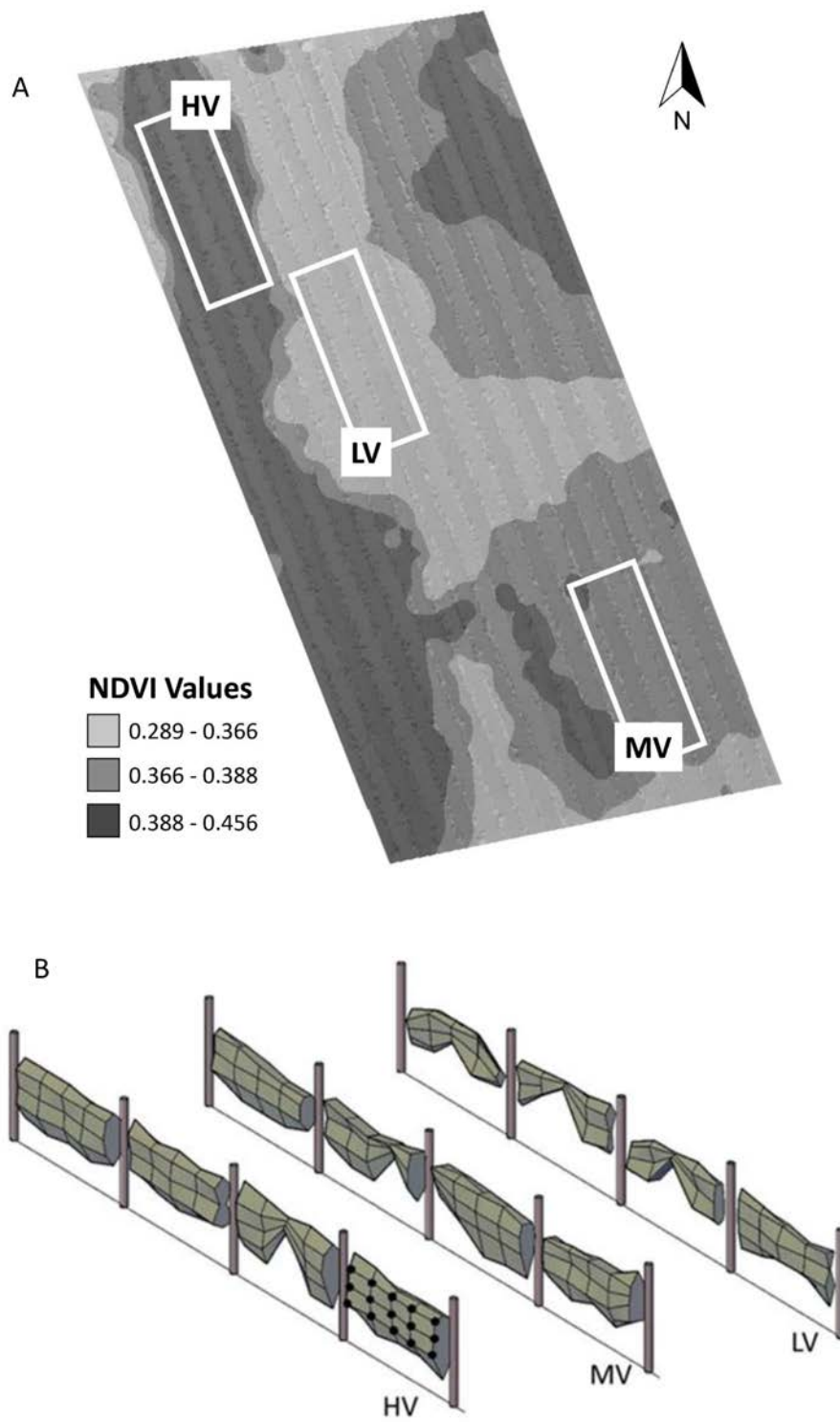
514

515

516

517

518

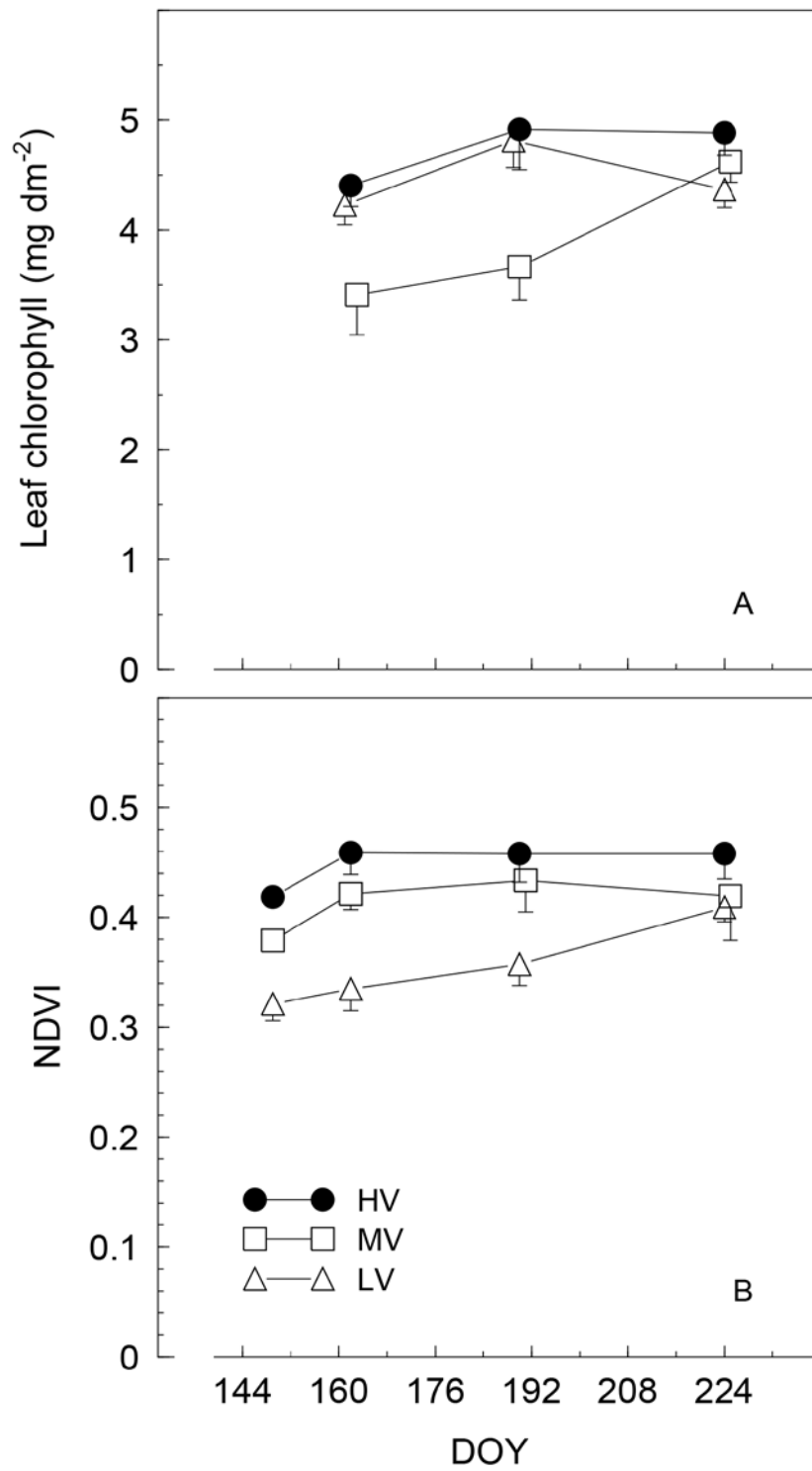


520

521

522

Fig. 1



524

525

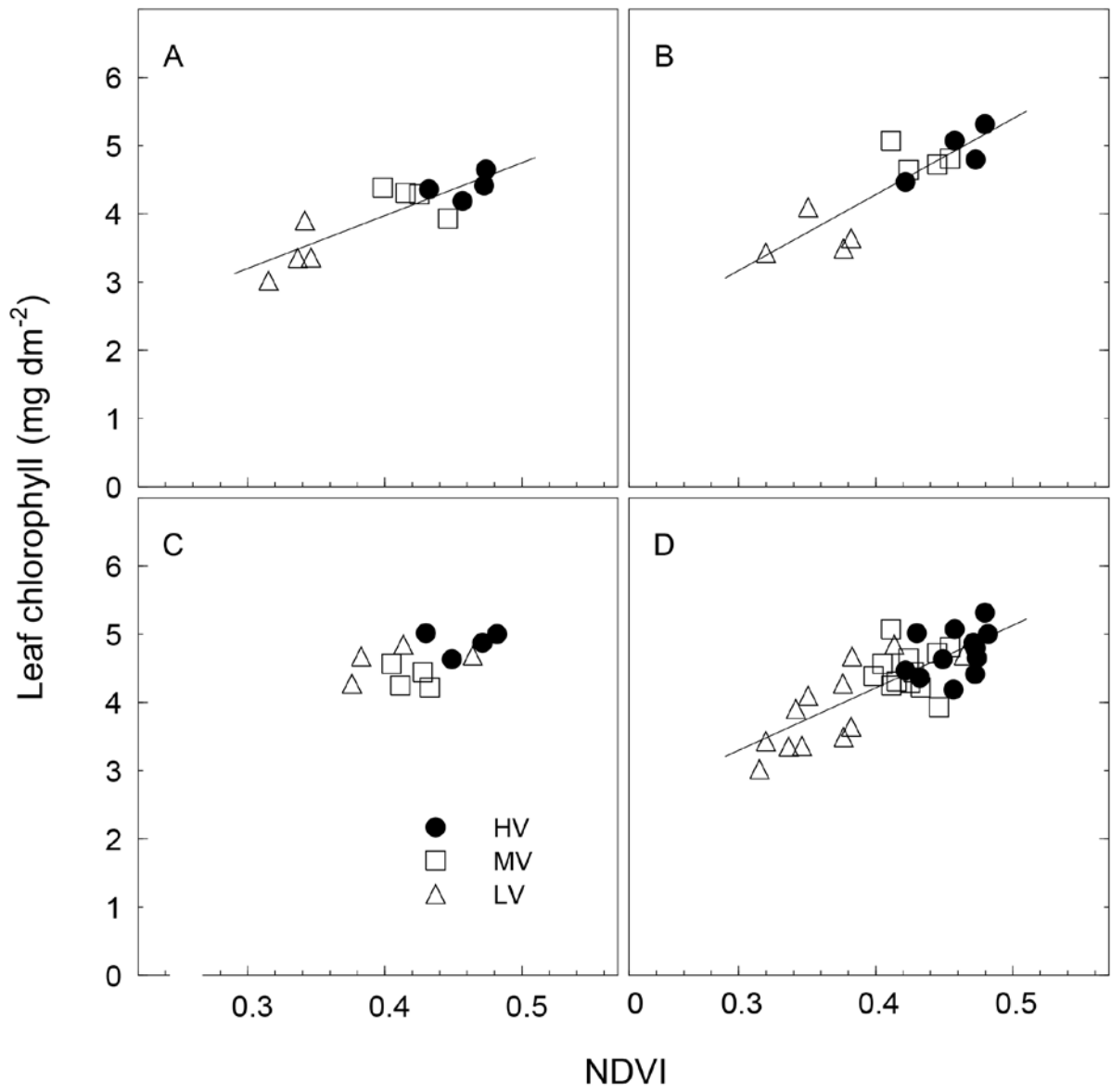
526

527

Fig. 2

528

529



530

531

532

533

534

535

536

537

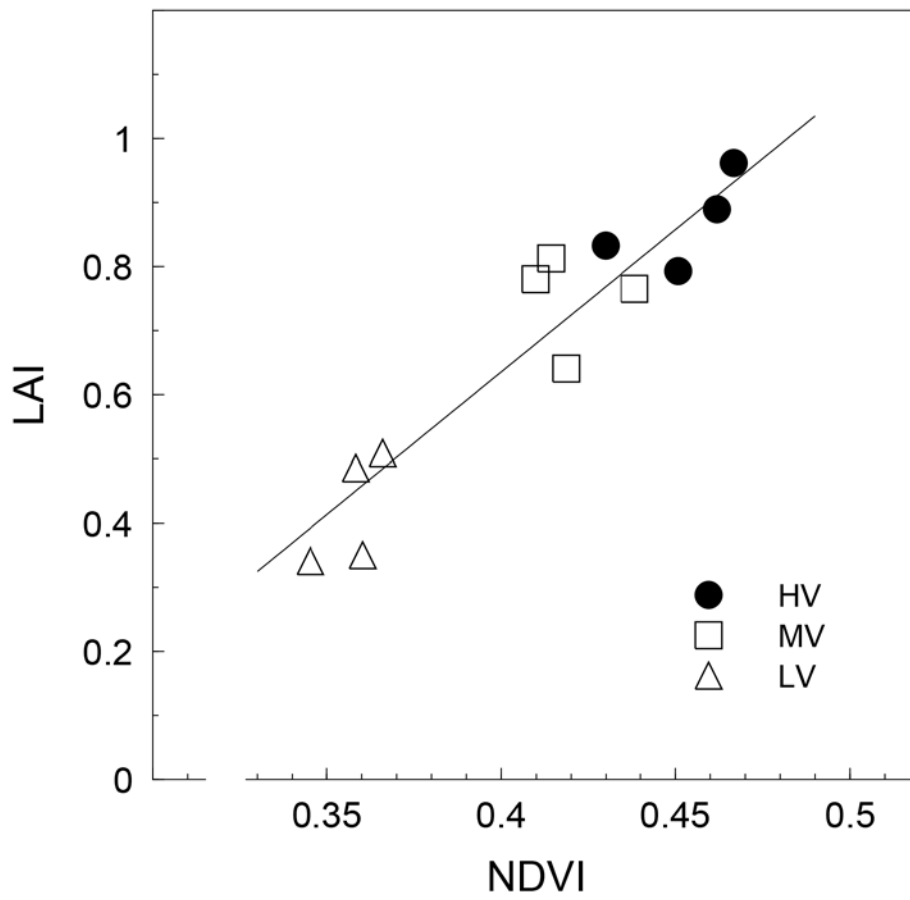
538

539

Fig. 3

540

541



542

543

544

545

546

547

548

549

550

551

552

553

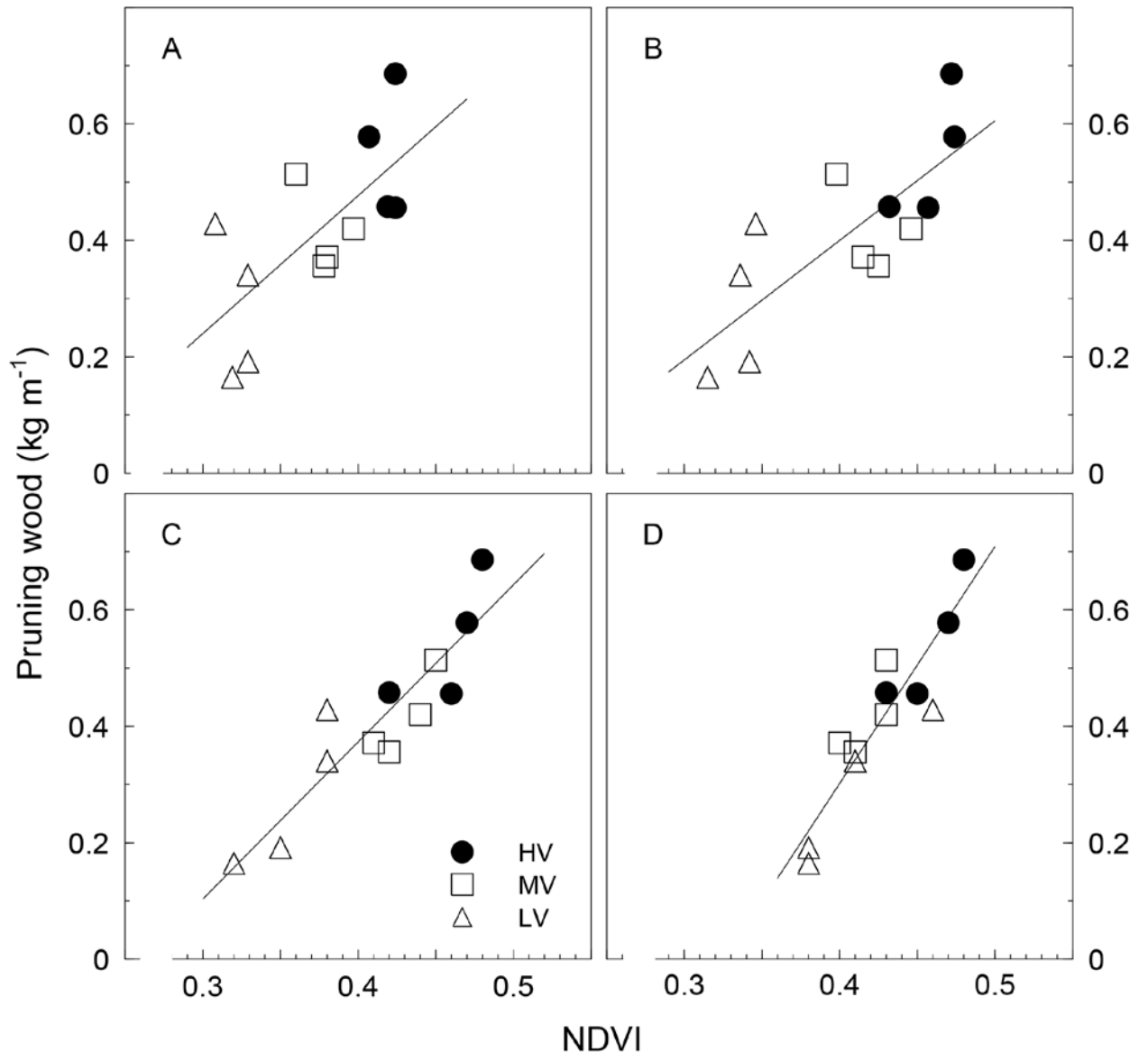
554

555

Fig. 4

556

557



558

559

560

561

562

563

564

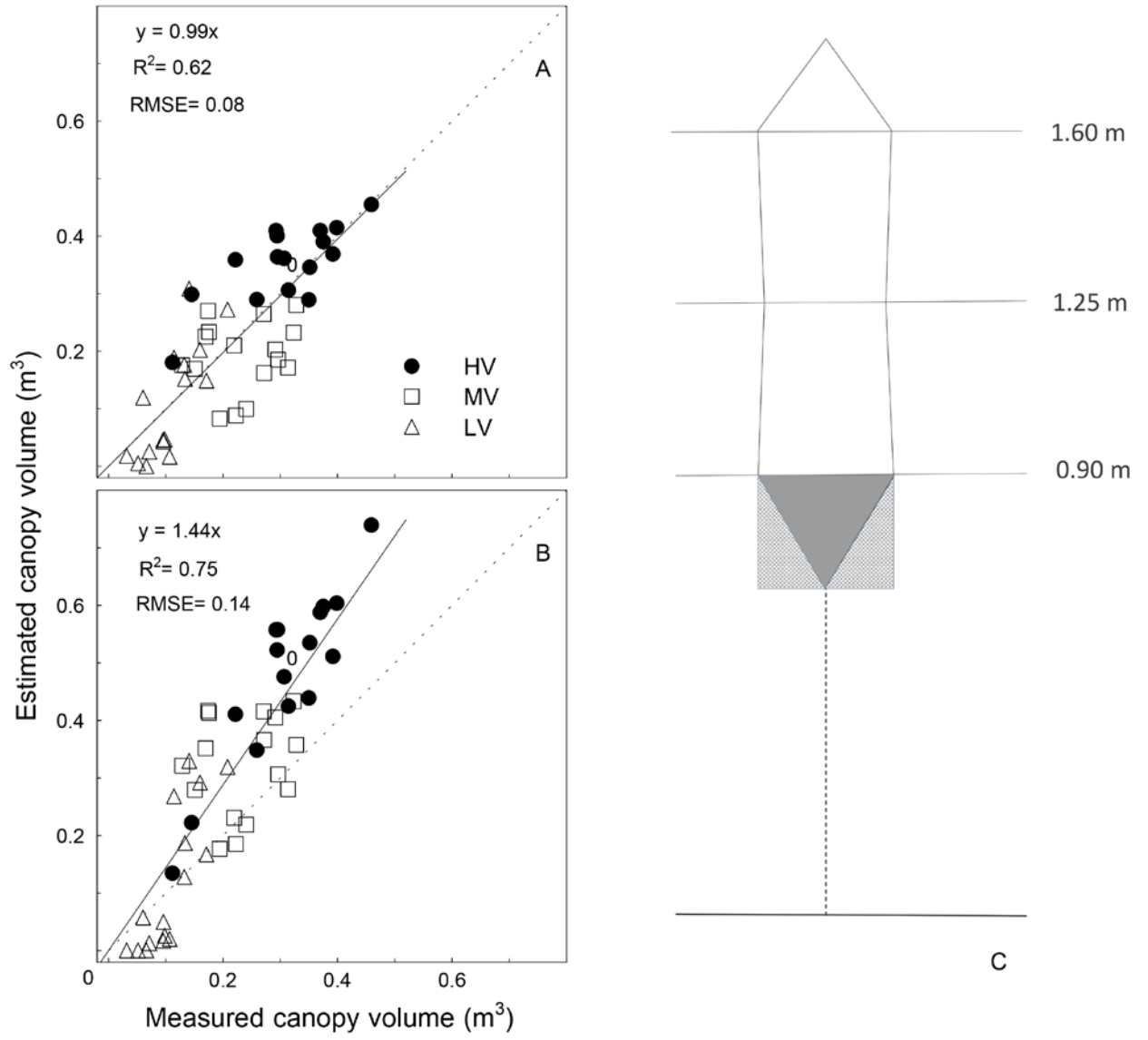
565

566

567

Fig. 5

568
569
570

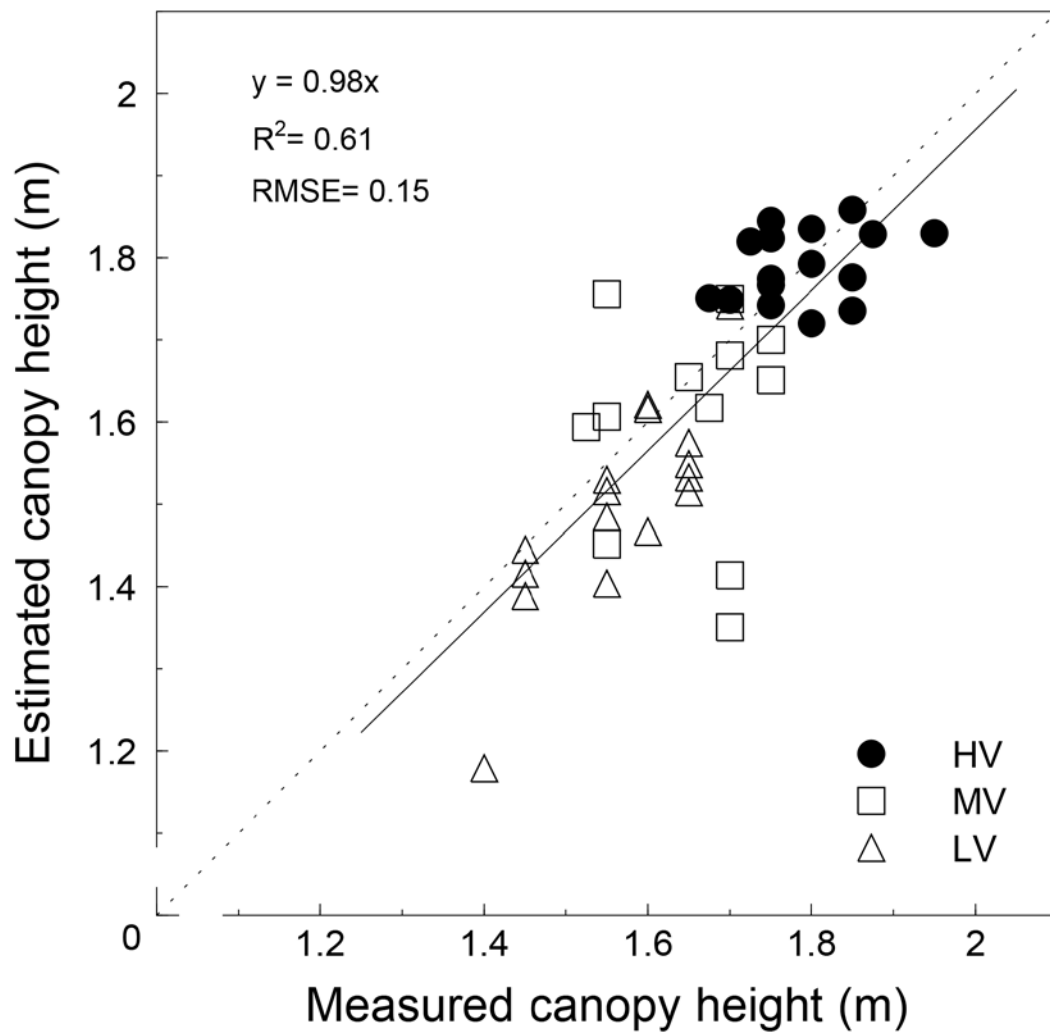


571
572
573
574
575
576
577
578
579

Fig. 6

580

581



582

583

584

Fig. 7

585

586

587

588

589

590

591

592